Directional Emittance of a Two-Dimensional Ceramic Coating

W. D. TURNER*
Texas A & I University, Kingsville, Texas
AND
T. J. LOVE†
University of Oklahoma, Norman, Okla.

The results of a numerical study using Monte Carlo techniques are presented illustrating the effects of various optical parameters on the directional emittance near the edge of a ceramic coating. The model includes scattering and Fresnel reflections at the bounding surfaces. Effects of refractive index and optical thickness for two scattering albedos are examined for properties typical of ceramic materials. It is noted that corner effects appear to be significant only within one-dimensionless optical distance from the edge of the material.

Nomenclature

A	=	generating area ($SOL \times L$)
H	=	semi-infinite strip width
I	=	intensity of thermal radiation
I_{bb}	=	blackbody intensity
L	=	slab thickness
n	=	refractive index
N	=	total number of emissions
$N(\mu',\varphi')$	=	number of emissions through a selected area
PL	=	path length
R	=	uniform random number
SOL	=	slab optical length
X,Y,Z	=	system coordinates
x,y,z	=	emissions coordinate system
y',z'	=	translated coordinates
β	=	extinction coefficient
ϵ	=	emittance
θ_c	=	critical angle of incidence
θ_F	=	Fresnel angle of incidence
$\varkappa$	=	absorption coefficient
μ'	=	cosine of escape polar angle
ρ	=	reflectivity
σ	=	scattering to extinction ratio (albedo)
τ	=	optical thickness
φ	=	azimuthal angle
φ'	=	escape azimuthal angle
ω	=	solid angle

I. Introduction

THE usage of coatings for temperature control of surfaces has widespread application today. Most of the published literature deals with painted coatings, using selected pigments to achieve the desired physical and optical properties. A great deal of research is concerned with the performance of these pigmented coatings after exposure to atmospheric and solar conditions. Less information is available about ceramic coatings and their properties. The principal references in this area are the reports of Folweiler.[1] These reports are both theoretical and experimental, listing such data as scattering coefficients, absorption coefficients, transmittance, and normal emittance for samples of aluminum oxide and other ceramic materials. There is a large variation between some of the measured and calculated data; therefore, the results are used only to establish the general range of optical conditions used in this directional emittance study.

The geometry considered is that of a semi-infinite slab that absorbs, emits, and scatters thermal radiation. Isotropic scattering is assumed, and the effects of multiple scattering are included. The scattering centers may be either voids or particles suspended in the solid matrix. The method of analysis is similar to Ref. 2 with the addition of Fresnel reflections at the boundaries.

Monte Carlo techniques are used to obtain the solutions for the directional emittance. The application of Monte Carlo methods in the analysis of coatings is not new. References 3 and 4 both used statistical approaches to determine optical characteristics of pigmented coatings. Both approaches, however, are concerned with infinite coating geometries. No previous solution for the directional emittance of a two-dimensional coating considering Fresnel reflectivities at the boundaries has been published. This study is intended to show the effects of optical thickness, refractive index, and scattering albedo on the directional emittance of a ceramic coating.

II. Monte Carlo Method

The geometry considered is shown in Fig. 1. Fresnel reflectivities are included at the edge and both the top and bottom surfaces. The coordinate system, generation of coordinates, and emission direction angles are shown in Fig. 2. The energy bundles are generated within the planes $SOL \times L$. The length SOL depends on the optical properties of the medium and represents a distance approximately equal to twice the average expected travel of an energy bundle. This average distance of travel was determined by following many individual histories for each optical condition. The collection length is approximately equal to half of the generating length, SOL.

The theory concerning probability density functions and their application to the solution of radiative heat-transfer problems by Monte Carlo methods is discussed in depth by

Presented as Paper 70-67 at the AIAA 8th Aerospace Sciences Meeting, New York, January 19–21, 1970; submitted August 13, 1970; revision received October 9, 1970.

* Assistant Professor of Engineering.
† Professor and Director, School of Aerospace, Mechanical and Nuclear Engineering.

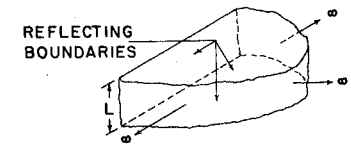

Fig. 1 Geometry analyzed.

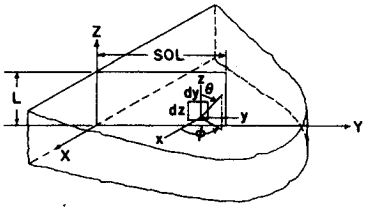

Fig. 2 Coordinate geometry.

Howell and Perlmutter[5] and will not be repeated here. The emission coordinates, emission direction, and path length are given in Ref. 2 but will be restated:

Coordinates

$$y = R_1 \times (SOL)$$

$$z = R_2 \times L$$

Emission Direction

$$\text{azimuthal angle } \varphi = 2\pi \times R_3 (0° \leq \varphi \leq 360°)$$

$$\text{polar angle } \cos\theta = 1 - 2R_4 (0° \leq \theta \leq 180°)$$

Path Length

$$\text{path length } PL = -(1/\beta) \ln R_5$$

R_1 through R_5 are random numbers.

If a scattering occurs at the end of the generated path length, the translated coordinates are determined by

$$y' = y + PL \times (\sin\theta \sin\varphi)$$

$$z' = z + PL \times (\cos\theta)$$

A new emission direction is determined as before.

The Fresnel-reflecting boundaries add an angular dependence to the radiation which escapes the medium. Radiant energy incident on the boundaries at an angle greater than the critical angle will be totally reflected, whereas energy incident within the critical angle cone will be reflected in accordance with Fresnel's equations. The critical angle θ_c is given by

$$\theta_c = \text{arc } \sin(1/n)$$

The polarization of the energy is not taken into consideration, and the reflectivity of the surface is commonly assumed to be one-half the sum of the parallel and perpendicular components of the electromagnetic energy. This is discussed by Love[6]:

$$\rho = [(n-1)/(n+1)]^2$$

Since a portion of the energy is transmitted and a portion is reflected for each energy bundle incident within the critical angle cone, this requires that a fraction of the energy be accounted for in each escape. This type of accounting is not pleasing and may be eliminated by a Monte Carlo decision. Since the reflectivity varies between 0 and 1, it may be compared directly with a random number varying uniformly between 0 and 1. The Fresnel reflectivity is calculated for each energy bundle and compared with a random number. If the random number is less than or equal to the value of the Fresnel reflectivity, the energy bundle is assumed to be totally reflected at that boundary location. If the random number is greater than the Fresnel reflectivity, the energy is completely transmitted. For instance, for a refractive index of 1.5 and normal incident energy, 0.96 of the energy is transmitted and 0.04 of the energy is reflected. If 100 bundles of energy are considered, 96 would, on the average, be transmitted by Monte Carlo decisions, and 4 would be totally reflected. For a large number of histories, the method should converge to the correct value of energy escaping the coating for each location.

If an energy bundle escapes from the coating, its escape polar angle, azimuthal angle, and location are determined. The escape polar angle θ' is determined from Snell's Law:

$$\sin\theta' = n \sin\theta_F$$

The incident, reflected, and exit energies are all assumed to lie in the same plane; therefore, the azimuthal angle measured from the X axis remains the same for a given energy bundle. The escape locations are shown in Fig. 3. Both the plane and the edge are divided into infinite strips of finite thickness, and an escape from the coating within the collection region will be from one of the semi-infinite strips. In addition, the azimuthal plane is divided into 12 sections for both the top and bottom planes and the edge. The number of polar angle divisions is 10. An escape is thus counted in one of the location strips, one of 12 azimuthal directions, and one of 10 polar directions. Symmetrical considerations reduce the total number of possible escape combinations, but the minimum number is 740 for the data obtained herein. The symmetry utilized included counting the top plane escapes in the appropriate bottom plane location, considering symmetry about the edge centerline, and considering symmetry about the Y axis for the plane surfaces and about the Z axis for the edge. The number of azimuthal divisions is thus reduced from 12 to 7.

The smaller polar divisions in the 70°–90° angular increment are necessary to define more closely the directional emission characteristics in this region. Since the coating is a dielectric, many of the large changes in curvature occur in this area.

After a sufficient number of histories has been followed to obtain the desired accuracy, the directional emittance is calculated from the following equation:

$$\epsilon(\mu',\varphi') = I(\mu',\varphi)/I_{bb(v)}$$

The blackbody intensity within the coating is given by

$$I_{bb(c)} = N/4\pi\kappa A$$

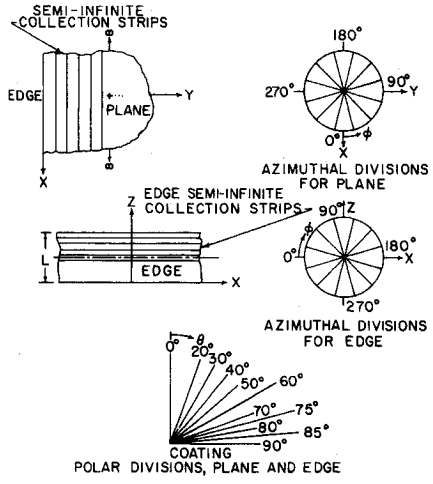

Fig. 3 Collection areas for two-dimensional solution.

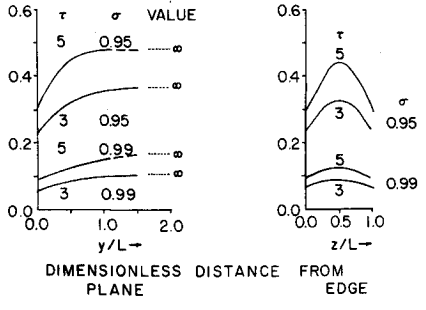

Fig. 4 Coating normal emittance for edge and plane.

Since the problem is two-dimensional, the emission generation reduces from energy per unit volume to energy per unit area. A is the area of the generating plane $SOL \times L$.

The directional intensity is found from the number of escapes for a given location within a given solid angle:

$$I(\mu',\varphi') = [N(\mu',\varphi')]/\cos\theta_{av}H\Delta\omega$$

Because the problem is two-dimensional, H reduces from an area to the width of the semi-infinite strip. $\text{Cos}\theta_{av}$ is the average of the polar angle within the solid angle $\Delta\omega$. The blackbody intensity in a vacuum differs by a factor n^2 from the intensity within the coating[6]:

$$I_{bb(v)} = (1/n^2)I_{bb(c)}$$

The directional emittance is thus found as follows:

$$\epsilon(\mu',\varphi') = n^2 4\pi A\kappa N(\mu',\varphi')/\cos\theta_{av}H\Delta\omega N$$

III. Results

The results for the directional emittances are obtained for two optical thicknesses, $\tau = 3$ and 5, two scattering albedos, 0.95 and 0.99, and a refractive index of 1.4. An optical depth of 3 corresponds to a coating thickness of approximately 0.006 in. using a nominal value of 200/cm for the extinction coefficient. The scattering albedos found by Ref. 1 for various ceramic coatings varied from 0.95 to 0.999+. For the nominal extinction coefficient of 200/cm, a scattering albedo much greater than 0.99 would result in very small values of the directional emittance (for the optical depths considered) and is thought to be of lesser importance. For this reason, the upper and lower limits on the scattering albedo are chosen as 0.99 and 0.95, respectively.

The normal emittance results for both the edge and the plane are shown in Fig. 4. The plane emittances are determined at a distance up to 1.5 optical thicknesses from the edge for $\tau = 3$, and up to 1.1 optical thicknesses for $\tau = 5$. The infinite values shown in Fig. 4 are the results for the normal emittance from a one-dimensional coating study for the same optical conditions. The normal emittance curve for $\tau = 5$, $\sigma = 0.95$ has essentially reached infinite conditions at a distance of one optical thickness from the edge. The other curves will reach infinite conditions at distances of approximately 1.5 to 2 optical thicknesses from the edge.

The value of the normal emittance increases with an increase in both optical thickness and absorption coefficient.

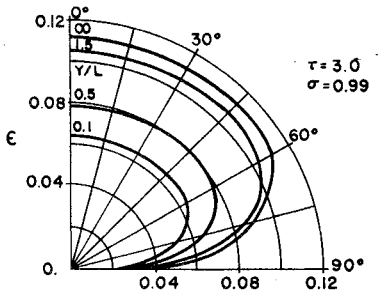

Fig. 5a Two-dimensional coating plane emittance: $\tau = 3.0$, $\sigma = 0.99$.

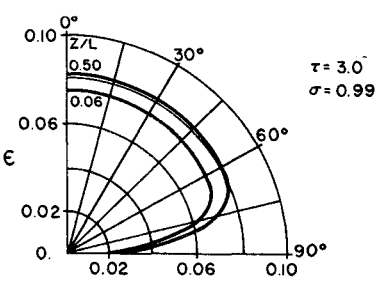

Fig. 5b Two-dimensional coating edge emittance: $\tau = 3.0$, $\sigma = 0.99$.

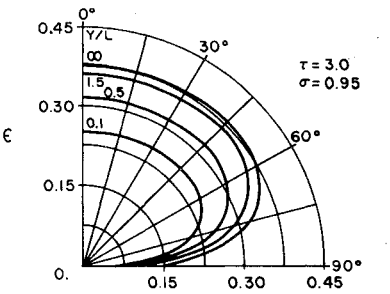

Fig. 6a Two-dimensional coating plane emittance: $\tau = 3.0$, $\sigma = 0.95$.

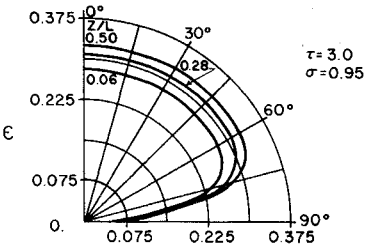

Fig. 6b Two-dimensional coating edge emittance: $\tau = 3.0$, $\sigma = 0.95$.

The curves for a scattering albedo of 0.95 are directional, showing an extreme dependence on location near the edge. The curves for $\sigma = 0.99$ are much flatter. The same general characteristics are observed for the edge. The normal emittance curves between $y/L = 0$ and 0.5 for the plane are very similar to the edge curves between $z/L = 0$ and 0.5.

In the analysis of the plane directional emittance, an unexpected result was found. The various emittances did not exhibit an azimuthal dependence. The data are collected in three dimensions, including seven azimuthal directions, but the emittance turned out to be a function only of polar angle and location. These results are shown in Figs. 5–8 for the four optical conditions tested. The $y/L = \infty$ curves shown in Figs. 5a, 6a, 7a, and 8a are from the one-dimensional data for the same optical conditions. It may be seen that the curve shape for $y/L = \infty$ is very similar to the directional emittance curves at $y/L = 1.0$ and 1.5. This is particularly evident in Fig. 8a, where the coating emittance at $y/L = 1.0$ has essentially reached infinite conditions. The two curves differ by no more than 3% at any point, and this type of agreement is within the accuracy of the Monte Carlo program; it may be concluded, therefore, that infinite conditions have been reached for the plane at this distance.

Edge emittance curves have essentially the same shape, and they, too, are azimuthally independent. The edge directional emittances are shown at $z/L = 0.06$, the closest distance from the plane possible in the program, $z/L = 0.28$ (except for Fig. 6b), and at the edge centerline, $z/L = 0.5$.

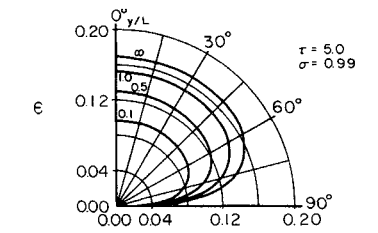

Fig. 7a Two-dimensional coating plane emittance: $\tau = 5.0$, $\sigma = 0.99$.

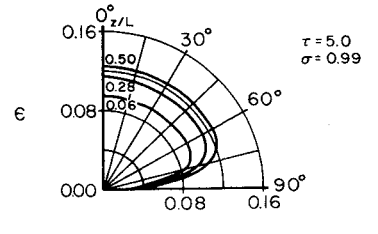

Fig. 7b Two-dimensional coating edge emittance: $\tau = 5.0$, $\sigma = 0.99$.

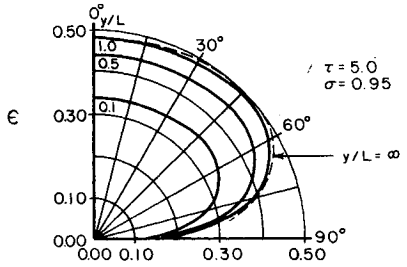

Fig. 8a Two-dimensional coating plane emittance: $\tau = 5.0$, $\sigma = 0.95$.

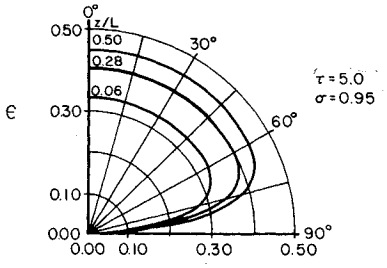

Fig. 8b Two-dimensional coating edge emittance: $\tau = 5.0$, $\sigma = 0.95$.

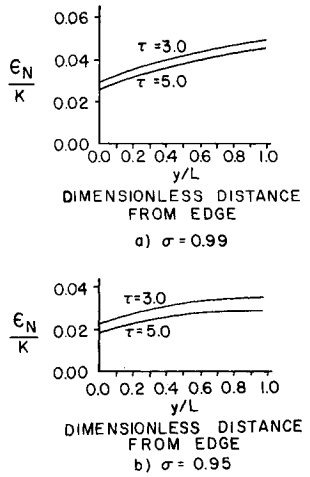

Fig. 9 ϵ_N/k for two-dimensional coating.

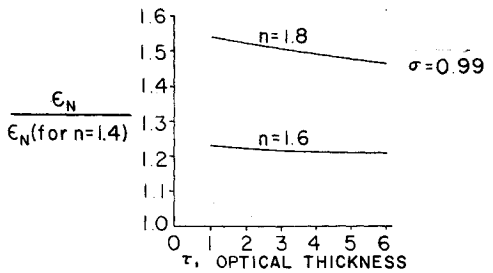

Fig. 10a Increase in normal emittance as a function of refractive index and optical thickness: $\sigma = 0.99$.

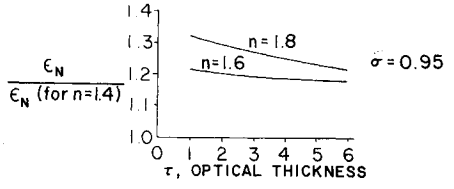

Fig. 10b Increase in normal emittance as a function of refractive index and optical thickness: $\sigma = 0.95$.

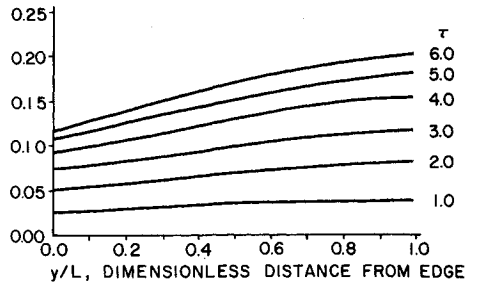

Fig. 11 Normal emittance of plane for various optical thickness: $n = 16$, $\sigma = 0.99$.

The original purpose of the study was to determine the effects of refractive index, optical thickness, and absorption coefficient on the directional emittance of a ceramic coating. Since the amount of IBM 360/40 computer time required to obtain a complete two-dimensional solution is approximately 20 hr, only the four different solutions have been run. However, correlations have been found between the one-dimensional and two-dimensional solutions which related the effects of refractive index and optical thickness to the normal emittance.

The two correlations used involved the relationship of normal emittance to absorption coefficient, $\epsilon_N/\varkappa$, and the change in normal emittance as a result of changes in refractive index for $\sigma = 0.95$ and 0.99. The increase in normal emittance for a scattering medium is proportional to the optical thickness. For a very high scattering medium such as one having a scattering albedo of 0.999, an increase in the optical thickness from one to three increases the normal emittance nearly a factor of three. As the scattering albedo is decreased, the percent increase in normal emittance is smaller when the optical thickness is increased. The $\epsilon_N/\varkappa$ data are plotted for the two-dimensional coating in Fig. 9. The difference in the curves for $\tau = 3$ and $\tau = 5$ remains fairly constant up to one optical thickness from the edge. Using the one-dimensional results from Ref. 7 to determine the percent changes in normal emittance for optical thicknesses of one, two, three, four, five, and six, the various $\epsilon_N/\varkappa$ curves are constructed for the two-dimensional coating. From these curves, the extended results for a refractive index of 1.4 are obtained.

To complete the analysis, the change in emittance as a function of refractive index changes must be determined. Figure 10, obtained from the one-dimensional data, shows the increase in normal emittance (using the emittance for $n = 1.4$ as a base) as a function of optical thickness for refractive indexes of 1.6 and 1.8. The extended analysis results for $n = 1.6$ and 1.8 are then obtained using Fig. 10.

Some of the two-dimensional extended results are shown in Figs. 11–14. These figures give the normal emittance as a function of location for various optical thicknesses and refractive indexes for the two scattering albedos, 0.95 and 0.99. Reference 7 contains all of the extended results obtained in the study. After the value of the normal emittance is obtained from the proper optical condition, the directional

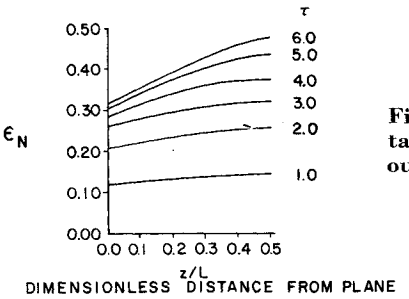

Fig. 12 Normal emittance of edge for various optical thicknesses: $n = 1.4$, $\sigma = 0.95$.

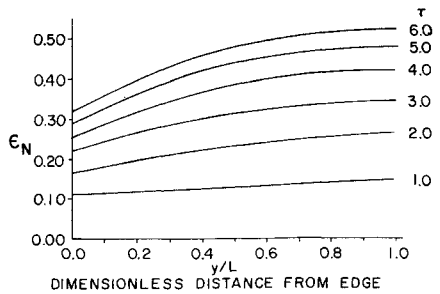

Fig. 13 Normal emittance of plane for various optical thicknesses: $n = 1.4$, $\sigma = 0.95$.

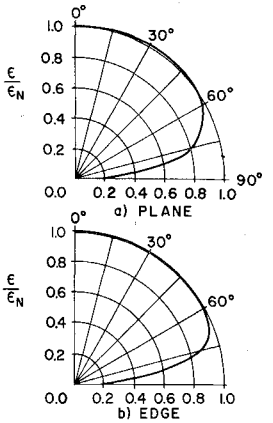

Fig. 15 Composite curves of ϵ/ϵ_N for edge and plane emittance.

emittance curve is found using the composite results of Fig. 15. These curves were obtained by plotting all of the two-dimensional results and drawing a best-fit curve through the data. Using the complete extended normal emittance data contained in Ref. 7 and the composite curves, the directional emittance can be obtained for any optical thickness between one and six and for a refractive index between 1.4 and 1.8, for the two scattering albedos.

In calculating the extended data, it is assumed that the one-dimensional changes in emittance as a function of refractive index and optical thickness are applicable to the continuous normal emittance of the two-dimensional problem. There is also some variation in the emittance curve as a function of optical thickness and refractive index, particularly for small optical thicknesses. These differences are primarily in the curvature in the 60°–90° polar region of the emittance curve. It is assumed, however, that the normalized emittance curves are similar enough for the results of composite curves such as Fig. 15 to be meaningful.

IV. Conclusions

The following briefly summarizes the results and conclusions from the analysis:

1) For the two scattering albedos studied, the emittance increased with an increase in either optical thickness or refractive index.

2) Both the edge and the plane directional emittances are azimuthally independent.

3) The emittances are directional and are dependent on both locations and polar angle.

4) Emittances showed a location dependence only for short distances from the edge, usually one to two optical thicknesses.

5) Normal emittance curves for $\sigma = 0.99$ are much flatter than the $\sigma = 0.95$ emittance curves.

Comment 4 perhaps deserves a little more discussion. An optical thickness of 5 and a scattering albedo of 0.95 produced essentially infinite conditions at a distance of one optical thickness from the edge. Using the normal value of the extinction coefficient, 200/cm, this corresponds to a coating thickness of 0.010 in. In terms of these physical dimensions, the location directionality extends only one edge thickness or 0.01 in. from the edge. For such a coating, if the size is much greater than the thickness, the edge or location effects can essentially be ignored, and the coating could be analyzed as a one-dimensional problem.

The accuracy of the two-dimensional computed results is expected to be within ±5%, using a central limit theorem probability error analysis. The extended analysis results are more difficult to analyze in terms of a specific error, since an undetermined error is involved in the interpolation and extrapolation of the data. A reasonable estimate of the error limits for the extended data is ±10%.

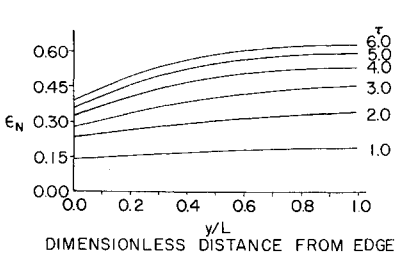

Fig. 14 Normal emittance of plane for various optical thicknesses: $n = 1.8$, $\sigma = 0.95$.

References

[1] Folweiler, R. C., "Thermal Radiation Characteristics of Transparent, Semi-Transparent and Translucent Materials under Non-Isothermal Conditions," Part I, April 1964; Part II, June 1964; Part III, March 1966, Lexington Labs., Cambridge, Mass.

[2] Love, T. J. and Turner, W. D., "Directional Emittance from Emitting, Absorbing, and Scattering Media," *AIAA Progress in Astronautics and Aeronautics, Thermophysics: Applications to Spacecraft*, Vol. 23, edited by Jerry T. Bevans, Academic Press, New York, 1970, pp. 319–334.

[3] Zerlaut, G. A., *Investigation of Light Scattering in Highly Reflecting Pigmented Coatings*, 1966, Vol. 1, "Summary Report"; Vol. 2, "Classified Investigations; Theoretical and Experimental"; Vol. 3, "Monte Carlo and Other Statistical Investigations," Illinois Institute of Technology, Chicago, Ill.

[4] "Infrared Diffuse Reflector Coating," 1st, 2nd, and 3rd Quarterly Progress Reports, July 1, 1966–April 1, 1967, Honeywell Systems and Research Division.

[5] Howell, J. R. and Perlmutter, M., "Monte Carlo Solution of Thermal Transfer through Radiant Media Between Gray Walls," *Journal of Heat Transfer*, Vol. C86, 1964, pp. 116–122.

[6] Love, T. J., *Radiative Heat Transfer*, Charles Merrill Books, Inc., Columbus, Ohio, 1968.

[7] Turner, W. D., "Directional Emittance of Emitting, Absorbing, and Scattering Media," Ph.D. dissertation, 1969, Univ. of Oklahoma, Norman, Okla.